Mechanical Systems and Signal Processing 49 (2014) 234–248

Contents lists available at ScienceDirect

Mechanical Systems and Signal Processing

journal homepage: www.elsevier.com/locate/ymssp

A radar-based monitoring of the Collserola tower (Barcelona)

G. Luzi *, M. Crosetto, M. Cuevas-González

Remote Sensing Department – Division of Geomatics, Centre Tecnològic de Telecomunicacions de Catalunya (CTTC), Av. Gauss, 7, E-08860 Castelldefels (Barcelona), Spain

ARTICLE INFO

Article history:
Received 8 October 2013
Received in revised form
20 March 2014
Accepted 23 April 2014
Available online 15 May 2014

Keywords:
Radar
Interferometry
Vibration
Tall tower
Cable force tension

ABSTRACT

This paper reports a set of experiments aiming at evaluating the capability of an innovative radar technique to measure the dynamic response of a 268 m high tower, the Collserola tower located in Barcelona, and its guys; the tension force of some guys is also estimated from the obtained vibration frequencies. The applied procedure was based on the use of a coherent radar system: temporal samples acquired using different observation geometries were processed to retrieve the vibration characteristics of both the tower and its guys. This was attained by observing the tower in a fully remote sensing mode, i.e. several hundred metres from the object, without installing any reflector on the tower, and under micro-tremor and wind-induced excitation. During the campaigns, which were spread over three years, the investigated technique demonstrated its capability to measure the dynamic response for a number of different points of the tower with high repeatability. The performed experiments also allowed distinguishing and characterizing the different contributions of the tower and the guys.

1. Introduction

Articles focused on the use of microwave remote sensing to measure the dynamic response of a variety of structures, as bridges [1–3], buildings [4,5], wind farms [6], chimneys [7], ancient towers [8] and guyed masts [9] among others, have been widely disseminated in the last ten years. The capability to measure displacements with sub-millimetre accuracy and consequently, to identify the characteristics of key vibration modes, from distances up to hundreds of metres, and with negligible influence of the weather conditions, are major advantages of this technique. Although radar interferometry is only able to provide an estimate of the radar Line-Of-Sight (LOS) component of the actual displacement, it can contribute to understand the behaviour of complex structures, which is particularly useful when the use of contact sensors is costly or needs hazardous installations, as in the case of bridges, tall structures, guys, etc. In this paper, experimental results collected during three different monitoring campaigns are reported. The monitored structure is a tall tower located in the Barcelona neighbourhoods, namely the Collserola tower [10]. The data acquired using Ku-band real-aperture interferometric radar, with different observation geometries, are analysed to retrieve vibration characteristics of the structure and to estimate the tension force of the guys. The first experimental test was performed in 2008 but main data here analysed are from the following campaigns, carried out in 2012 and 2013.

The paper is organized in five sections. This brief introduction is followed by a short outline of the technique and the used radar sensor, and a description of the monitored structure. A selection of the data acquired in the last years is analysed

* Corresponding author. Tel. +34 936 452 900.
E-mail addresses: gluzi@cttc.cat, guido.luzi@gmail.com (G. Luzi).

http://dx.doi.org/10.1016/j.ymssp.2014.04.019
0888-3270/

with the following objectives: describing the spectral response of the tower, evaluating the repeatability of the discussed radar measurements, estimating the first mode shapes of the tower and finally retrieving the tension force of the guys from their resonant frequencies. A concluding section summarizes the outcomes originated from the study.

2. The radar technique and the sensors

The first studies based on the radar technique discussed in this work date back to the end of the 1990s [11,12]. The technique matured during the following years [13], until the availability of commercial instruments [14]. The data discussed in this paper were acquired through an industrially engineered radar interferometer, which consists of a coherent sensor, i.e. a radar able to provide both the amplitude and phase of the signal reflected by the investigated structure. We briefly recall the working principle of the technique, for a detailed description of the instrument see e.g. [2,14]. A radar measurement, using the time elapsed between the transmission and reception of an electromagnetic waveform provides a *range profile*: an amplitude signal composed by different peaks, which identify the main reflecting parts of the observed structure. Each point of this range profile, located at different distances, corresponds to sampling volumes, usually called radar bins. So, a real aperture radar observation has only 1-D imaging capabilities and only different targets which are placed at different distances from the radar can be unambiguously detected and a careful analysis of the range profile is mandatory to avoid errors due to the multiplicity of contributions coming from different points placed at the same distance from the radar; in Section 4, dedicated to the data collection, a clear example is illustrated.

The amplitude and phase values of the reflected signal are associated with different parts of the illuminated structure. The first one is related to the accuracy of the phase measurement and to the capability to detect different parts of the monitored structure. The phase information allows, through interferometry, evaluating range variation in terms of number of wavelengths of the propagating radar wave. When the displacement remains within $\pm\ \lambda/4$, being λ the wavelength of the transmitted wave, it is linearly related to the variation of distance $d_{LOS}(t)$ occurred between two successive radar acquisitions:

$$d_{LOS}(t) = \frac{\lambda}{4\pi} \cdot \Delta\varphi(t) \tag{1}$$

where $\Delta\varphi(t)$ is the difference between the phases measured in two successive radar acquisitions. The measured phase values are confined in the $(-\pi,+\pi)$ interval so to retrieve displacements larger than $\lambda/4$ we have to apply a correction procedure named phase unwrapping [15]. In conclusion, acquiring consecutive range profiles with sampling frequency up to 200 Hz, the displacement history (time series) of parts of the observed structures are available for its temporal and frequency dynamical behaviour. The achievable precision is a small fraction of the wavelength of the transmitted electromagnetic waves and depends on instrumental and experimental aspects [14].

The Centre Tecnològic de Telecomunicacions de Catalunya (CTTC) owns a commercial radar with interferometric capability: the IBIS-S, manufactured and marketed by IDS (Ingegneria dei Sistemi SpA). The system consists of a sensor module, a control PC and a power supply unit and data processing software. The maximum acquisition rate is 200 Hz, depending on the selected maximum range and decreasing as the maximum operating distance increases. Details on the radar equipment can be found in [14]. The sensor module transmits an electromagnetic signal at a central frequency of 17.2 GHz (Ku band) with a maximum bandwidth of 300 MHz, corresponding in the spatial domain to a range resolution of 0.5 m. Range resolution is here intended as the minimum distance necessary between two targets to be separated, i.e. seen as two different subsequent bins. Using this central frequency, which corresponds to a 1.743 cm wavelength in vacuum, allows the system to detect sub-millimetre displacements. The radar instrument is mounted on a tripod equipped with a rotating head to adjust the bearing of the sensor towards the investigated structure. The main sensor characteristics are summarized in Table 1.

It is of main concern to underline that the inteferometric technique can only estimate deflections $d_{LOS}(t)$ along the radar LOS. That is, given a generic three-dimensional displacement, $\vec{d}(t)$, the radar technique can only observe and hence estimate the projection of $\vec{d}(t)$ in the LOS. If $\vec{d}(t)$ is perpendicular to the LOS, the displacement vector $\vec{d}(t)$ cannot be observed by the radar.

Table 1
Main characteristics of the radar system.

Radar main characteristics	
Operating frequency	17.2 GHz
Max. distance	1000 m
Max. radiofrequency bandwidth	300 MHz
Max. sampling rate	200 Hz
Weight of the system	12 kg
Battery autonomy	5 h

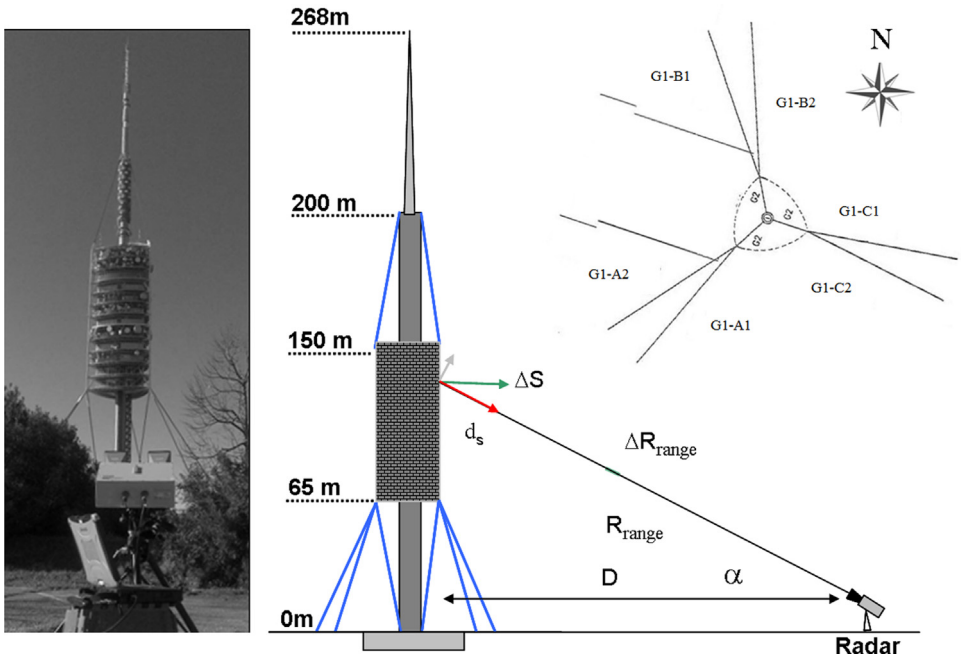

Fig. 1. View of the tower and the radar (left); scheme of the measurement geometry; plan view indication and name of the G1 cables (upper right).

The deflection measured by the radar concerns the relative range between the radar and reflecting surface. For this reason, in order to assure that the measured displacement can be ascribed to an actual motion of the reflecting surface, the possible vibrations of the sensor and its tripod have been properly considered. These vibrations can be estimated through specific experiments and they usually belong to the 7–12 Hz portion of the spectra [16]. In any case, in the study at hand, the tripod is installed in a stable area and its displacements are negligible with respect to those of the monitored structure. This permits to assure that the lower portion of the vibration spectrum (0.1–6 Hz), which is the most relevant to the study at hand, is not affected by the measuring system vibrations.

The location and dimension of the measured radar bins are dictated by the transmitting and receiving antennas field-of-view and by the range resolution. The antennas used in this work are two pyramidal horns whose half power beam-width in elevation and azimuth direction is 0.17 and 0.21 radians, respectively. The size of the illuminated area, which corresponds to an elemental sampling volume, is approximately 3 m^2 at 10 m range; this value increases as the observation angle, α, increases. The majority of the data here described were obtained using the mentioned high gain antennas (Gain = 23.5 dB) to improve the Signal-to-Noise Ratio (SNR) of the radar measurement. The bins that correspond to higher signal peaks are usually selected to analyse their displacement time series.

3. The monitored structure

The Collserola communications tower, designed by the architect Norman Foster, serves as a telecommunications tower for Barcelona and its neighbourhood [10]. It is one of the outstanding structures of the town, built in 1991 as part of an infrastructure upgrade to prepare the city for the Olympic Games of 1992. It stands from an altitude of 445 m a.s.l., reaching a maximum 266 m height above the ground and 286 m above its base, see Fig. 1. It is composed of five elements (structural sub-systems): concrete shaft, metal mast, block of platforms, pre-tensed metal guys and fibre guys. The concrete shaft is a column 205.5 m high with an annular section with a constant diameter of the inner space of 3 m. Its thickness varies: up to 162.5 m high is 0.75 m, corresponding to an external diameter of 4.5 m; in the following 18 m is 0.5 m; and in the rest is 0.3 m. The concrete shaft is topped by a cup, a metal piece. The metal mast is the natural prolongation of the concrete mast; it is a 34 m long, steel tubular mast, with a diameter of 2.7 m and 2.2 m at the lower and upper sections, respectively. It has an extension with a square-section lattice that is 37 m long, with a lower section measuring 1.5 m at the side and an upper section measuring 0.5 m at the side. At the top, a 7.5 m high crane is installed. The lower guys (G1 and G2) are steel cables, composed of a different number of strands (from 147 to 180 for each guy) and anchored to concrete blocks; the remaining ones (G3) are Kevlar fibre guys. The length of G1 varies from 83 m to 106 m, while G2 and G3 are 72.3 m and 58 m long, respectively. The block of platforms is a large metal structure whose base is in the form of an equilateral triangle of curved sides, 68 m height. It is anchored to the shaft at 12 points. The presence of a number of installed antennas (several hundreds of dishes, TV and FM operating) makes the facades of the service area highly heterogeneous from a mechanical point of view and with strong electromagnetic interference disturbances. A scheme of the tower is depicted in Fig. 2.

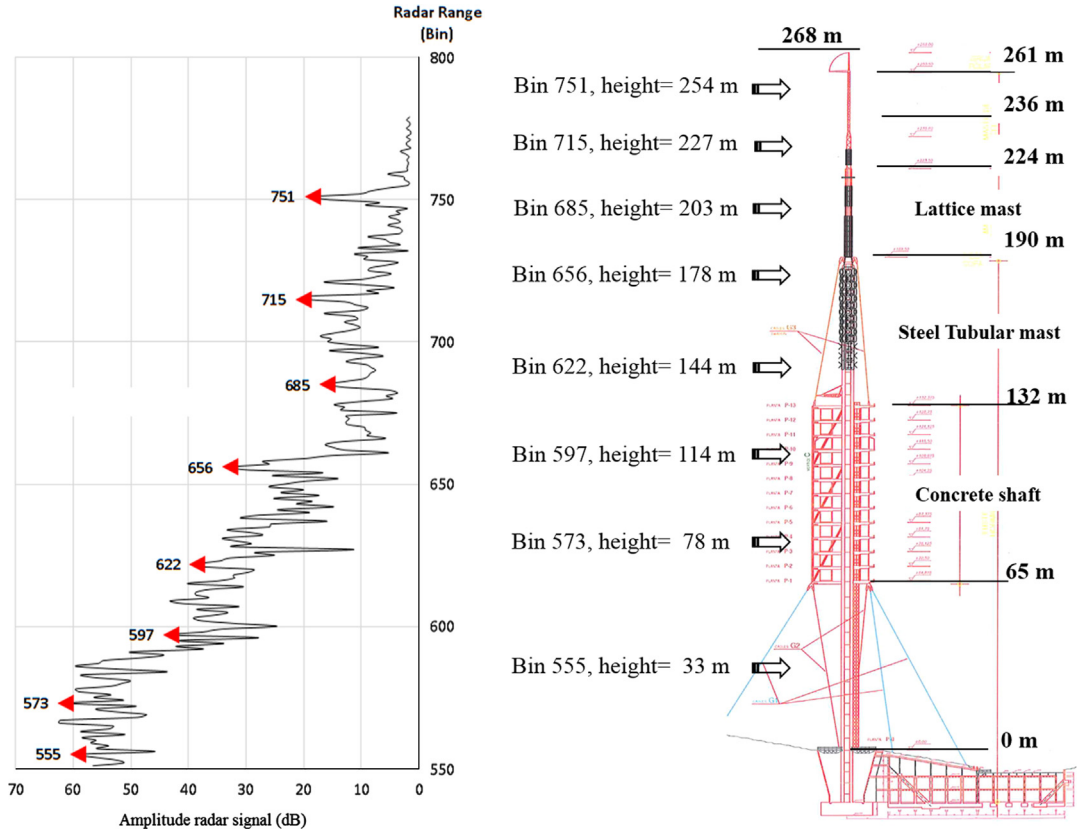

Fig. 2. Scheme of the tower (right) and an example of a range profile indicating a selection of radar bins (left). The part of the tower illuminated by the radar and the associated bins are indicated. Bins are selected among those with higher radar response and aiming at sampling the entire structure.

Table 2
Measuring configuration of the analysed experimental campaigns.

Measuring configuration	A1–08	B1–12	C1–13	C2–13	C2–13
Monitored structure	Tower	Guys	Tower	Tower	Tower
Date (dd/mm/yyyy)	02/10/2008	01/10/2012	13/02/2013	13/02/2013	13/02/2013
Starting time, local: (hh.mm)	14h29m GMT+2	11h21m GMT+2	10h44m GMT+1	12h10m GMT+1	13h28m GMT+1
Duration (s)	600	1800	3600	900	900
Sampling frequency (Hz)	40.01	98.95	40.63	16	16
Min distance to target (m)	266.5	16	275.5	620	800
Inclination angle (°)	37	36	29	12	27
Gain of antennas (dB)	20	23.5	23.5	23.5	23.5
Wind (m/s)/direction (°)	6.6/229	6.5/200	7/270	7/230	5/190

The structure generates very strong reflected signals from the radar point of view, thus assuring an elevated SNR even for acquisitions made at distances of hundreds of metres. This is essential to acquire and analyse radar samples corresponding to tens of points of the structure. It is worth noting that an analogous monitoring carried out with conventional contact sensors, e.g. accelerometers, would be unadvisable due to its high costs and the strong electromagnetic noise, which can totally compromise their functioning.

4. Data collection and analysis

The experimental results discussed in this paper were obtained in three campaigns with different measuring configurations, as summarized in Table 2. Basically two different geometries have been used to acquire the data here analysed. The first, aimed at monitoring the tower, is depicted in Fig. 1. In this case, the radar is located at different distances from the tower with an observation angle selected to illuminate the entire structure. In the scheme shown in Fig. 1, R_{range} is the distance between the radar and the reflecting point of the structure, D is the horizontal radar–target distance and α is the observation angle. The grey arrow indicates an example of displacement, ΔS, while the dark arrow represents the LOS

displacement component measured by the radar, d_s. An example of the range profile available from this geometry and a representation of the association between radar bins and tower sections are illustrated in Fig. 2.

The second configuration, illustrated in Fig. 3, is with the radar very close to a cable, observing it form different positions (referred as Q–Q4 in Table 2). In this case, the cable is clearly identified by the strongest peak in the range profile (see Fig. 3).

As far as the analysis of the data is concerned, the next chapter is divided as follows. The first section is dedicated to the detection of the main vibration frequencies of the tower. In the second section, the repeatability of the measurements is assessed by comparing data acquired from a fixed geometry at two different dates, and data collected within one day from three different locations and distances. Several results concerning the main vibration modes of the tower are reported in the third section. The above results together with a specific monitoring of the cables allowed separating the vibration frequency of the cables from those of the tower. Then, applying the simple taut string model, the cable frequencies were used to estimate the tensions. These aspects are described in the final fourth section.

4.1. Spectral response of the tower

The vibration frequencies of the monitored structure were derived by analysing the time series of displacements estimated from the radar interferometric measurements. The key step of the analysis was the computation of the power spectral density (PSD) using the Welch method [17], with 66% of overlapping sub-samples windowed by a Hanning function. Most of the temporal samples acquired during the 2013 campaign last 3600 s, a lapse which is approximately 1000 times larger than the previously measured period of vibration ($T=3.6$ s), guaranteeing a statistically robust sampling of the stationarity of the signal of interest. To evaluate the behaviour of the tower at different heights, the displacement time series of a set of 8 bins were selected and their PSD calculated. The correspondence between some bins and the associated parts of the tower is depicted in Fig. 2. The elemental sample volume corresponding to the radar bin in some cases also contains contributions from the guys: this issue will be taken into account in the analysis of spectral characteristics. Fig. 4 shows the (0.1–10 Hz) portion of the PSD of a 3600 s displacement time series, sampled at 40.63 Hz: the duration of the sub-samples was 500 s, resulting in a frequency resolution of 0.002 Hz. The lower part of the spectra is not shown due to the predominant contribution of instrumental noise ($1/f$ noise), while the signal at frequencies higher than 10 Hz maintains several orders of magnitude lower with respect to the detected peaks.

The PSD displayed in Fig. 4 shows three main peaks at 0.27 Hz, 0.474 Hz and 0.718 Hz. This is a common feature for all the bins. A further peak at 0.628 Hz is noticeable only for the bins corresponding to the central-lower part of the tower, i.e. for the bins 622, 597, 573 and 555. In particular bin 597, corresponding to the central part of the tower, shows a noisier spectrum: this is probably due to the complexity of the radar response of the illuminated area, which includes many independent vibrating targets (antennas). The area indicated with the circle is that one where the lower frequencies of the cables are located, as it will be described in detail in Section 4.4. It is important to point out that different types of vibrations can be distinguished by analysing multiple bins: the main body of the tower, the cables, and even the presence of additional noisy vibrating targets, like the antennas installed in the tower.

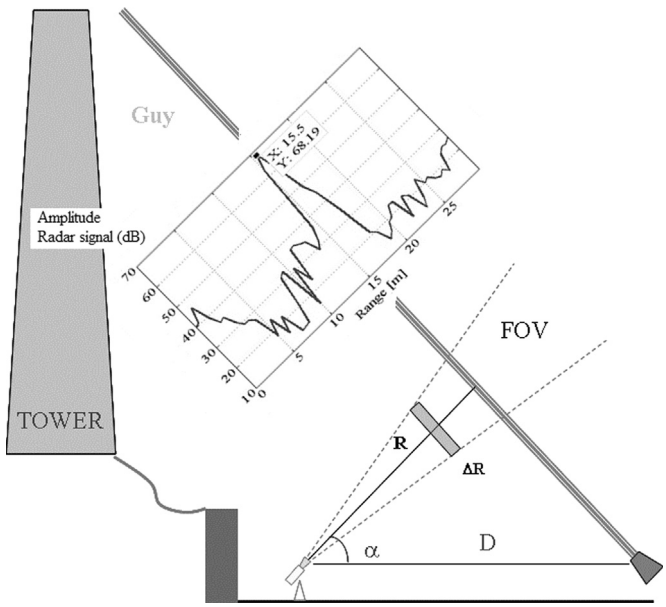

Fig. 3. Scheme of the measurement configuration (B1–12) aimed at monitoring cable G1–B2. The plot shows the radar profile, which displays a maximum at a distance of 15.5 m from the radar, in correspondence to the cable.

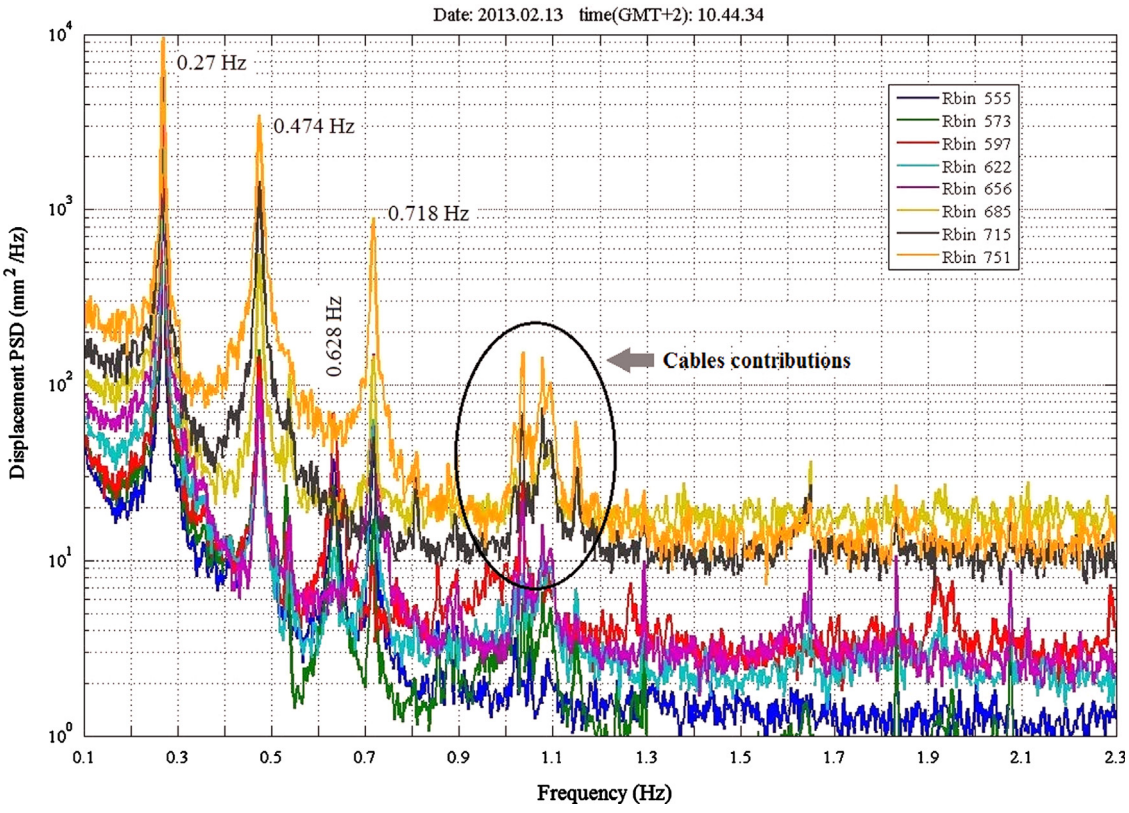

Fig. 4. Power spectral density (PSD) of the 01–2.3 Hz interval calculated with the Welch method for the displacement sample corresponding to the measurement configuration C1–13 (Table 2). Plots with different colours refer to different bins located at different heights of the tower. (For interpretation of the references to colour in this figure caption, the reader is referred to the web version of this paper.)

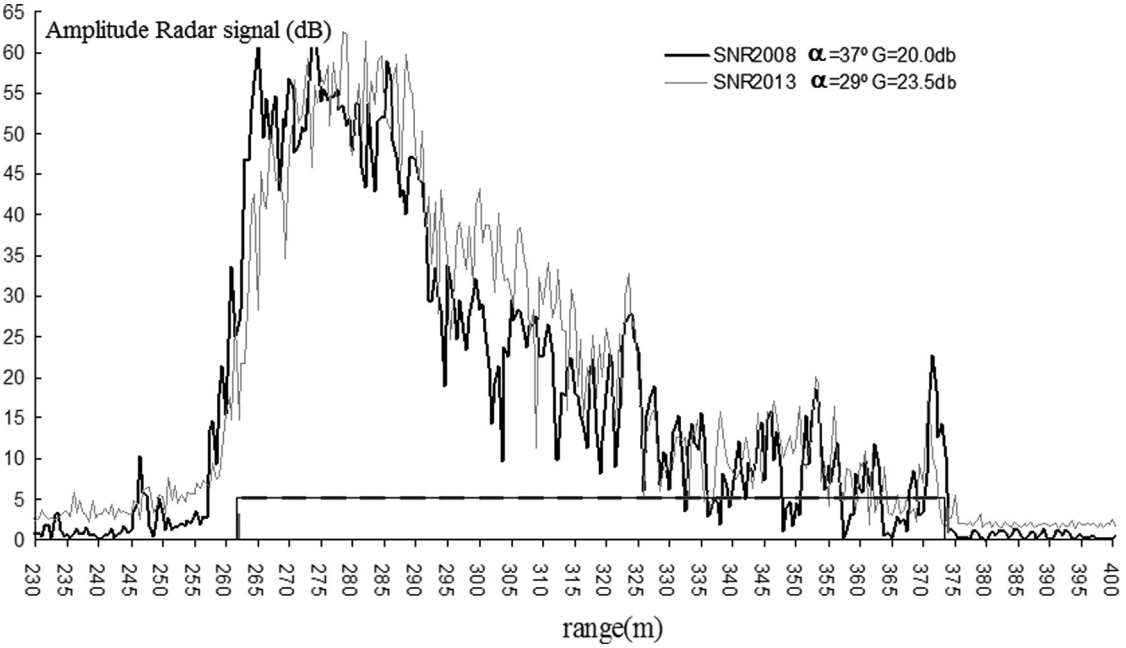

Fig. 5. Radar signal, configuration A1–08, using the antenna with a gain of 20.0 dB (black line) and configuration C1–13, using an antenna with gain of 23.5 dB (grey line).The rectangle on the *x* axis indicates the portion of the profile whose data correspond to tower points.

4.2. Repeatability of the radar measurements

Although the technique has been consolidated in the last few years through the results reported in several papers, only in a few cases measurements carried out at different times and from different distances have been compared to estimate the repeatability of the measurements. We assessed the repeatability by calculating the PSD from samples collected at different dates and distances. The first step involved a direct comparison between two radar range profiles, from which single bins for the spectral analysis were selected. Fig. 5 shows the range profiles acquired from the same radar position (configurations A1–08 and C1–13, see Table 2) with a five years lapse. In the second case, the antennas of the interferometer had a higher gain (23.5 dB), reducing the Field-Of-View (FOV) of the radar acquisition and improving the SNR of the acquisition. The observation angle slightly varied from 37° to 29°. Due to the smaller sampling volume and narrower FOV, the profile in the second case shows more details of the structure. However, despite the remarkable time separation, the two profiles of Fig. 5 are very similar.

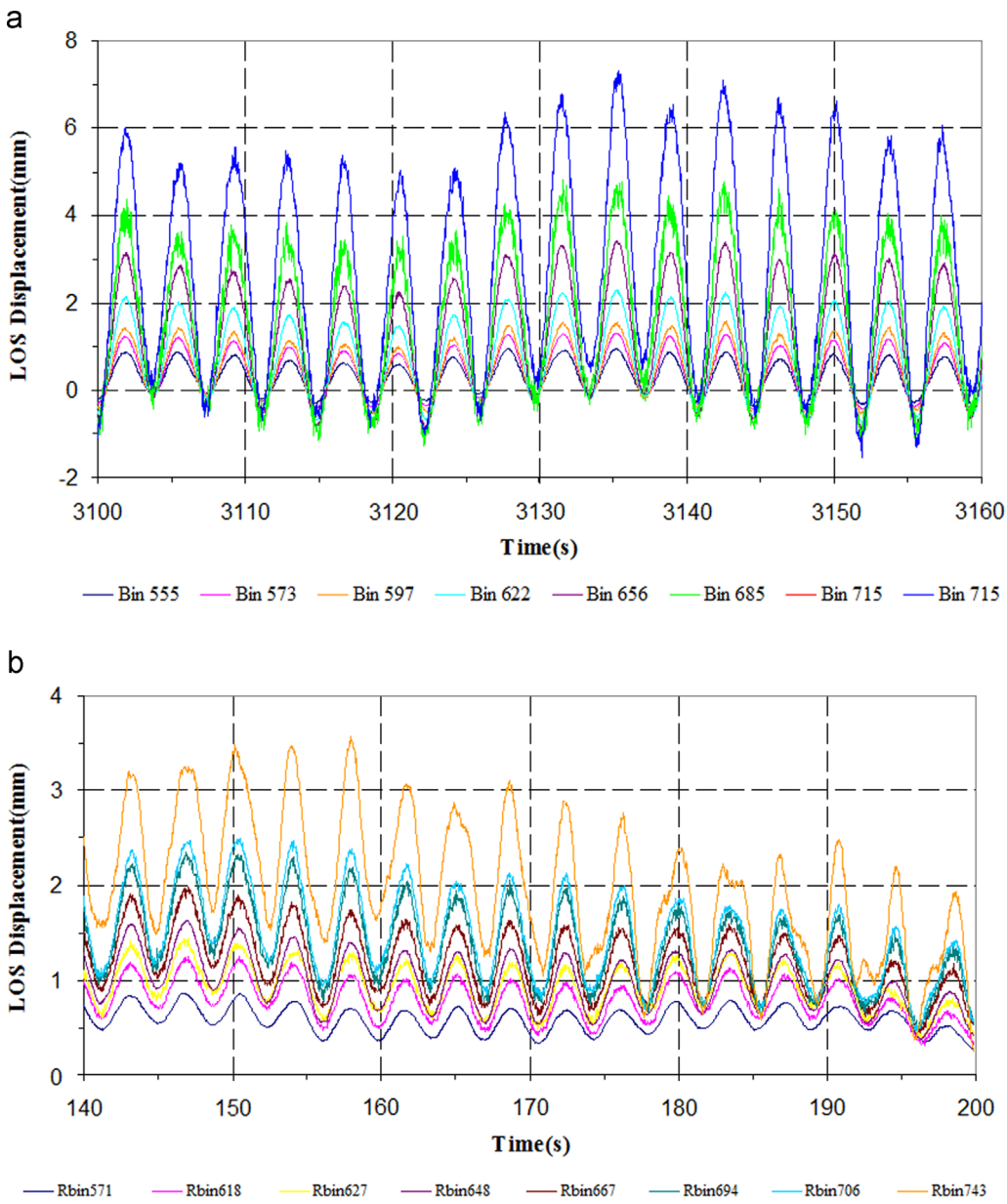

Fig. 6. LOS displacement time series retrieved from different radar measurements; different colours refer to different bins selected from the RAR power profiles and correspond to different heights of the tower. Configuration A1–08 (above) and configuration C1–13 (below). (For interpretation of the references to colour in this figure caption, the reader is referred to the web version of this paper.)

The similarity between the two signals proves that the environmental measuring conditions, as the atmospheric propagation or instrument instabilities, are of minor concern for radar acquisition. The two profiles have common features in correspondence to the higher peaks; for example, those located at bin 372, probably caused by some edge effect, overlap. Examples of the retrieved time series, acquired at the two dates, are depicted in Fig. 6. The different time series, which correspond to points distributed along the entire tower, are similar in shape and periodicity: they show amplitudes increasing with height with differences in the amplitude modules probably caused by the different wind conditions.

As far as the spectral characteristics of these data are concerned, a period of 3–4 s, is clearly noticeable directly from Fig. 6. Besides, accurate frequency values can be retrieved from the corresponding PSDs shown in Fig. 7. The first peak at 0.270 Hz coincides exactly, while the others differ less than 4% in the worst case. Considering that the 2008 sample was shorter, thus providing a PSD with lower frequency resolution (0.01 Hz), these values can be considered very similar.

To assess the operative limits of the sensor, the capability of the radar was tested operating at larger distances. An acquisition at 800 m from the tower (see configuration C2–13 in Table 2) was carried out. A displacement time series, which corresponds to the mid part of the tower, and its 60 s zoom are shown in Fig. 8. They show a periodicity analogous to the ones shown in Fig. 6. The main frequency value corresponding to Fig. 6 is 0.267 Hz, while the estimable value from Fig. 8 is 0.263 Hz. The difference of these two values is relatively small when compared with the frequency resolution of the PSD calculation (± 0.002 Hz). With respect to the previous data, as expected, the signal is a little bit noisy due to a lower SNR available from larger distances in radar measurement.

However, this does not prevent the correct estimation of the tower vibration characteristics. Analysing the data, in the first plot of Fig. 8, where a time interval of 900 s is shown, there is a remarkable but not critical influence of the atmospheric effects on the displacement measurements. This effect introduces smooth trends in the displacement time series, which are proportional to the sensor-to-target distance. It is worth underlining that these effects have no impact on the retrieval of spectral properties because they are easily removable during the data analysis [16]. The frequency values obtained during three different experimental campaigns (see details in Table 2) from 2008 to 2103 are summarized in Table 3. The value obtained for the main mode, f_0, is the more stable, within the error expected from PSD calculation (± 0.002 Hz), while a quite higher dispersion is shown by the highest frequency, f_3. The three measurements were obtained using displacement time series acquired with a slightly different sampling frequency (see Table 2).

4.3. Experimental estimation of the mode shapes of the tower

The availability of a large number of simultaneous displacement samples, corresponding to different points of the structure, also provided the opportunity to estimate the main modal shapes of the structure by using the FDD (Frequency Domain Decomposition) method [18]. We processed data corresponding to two set of data: measurements C1–13 and A1–08 (see Table 2). Three vibration modes were clearly identified in the frequency interval 0.0–1.0 Hz: 0.26 Hz, 0.475 Hz and

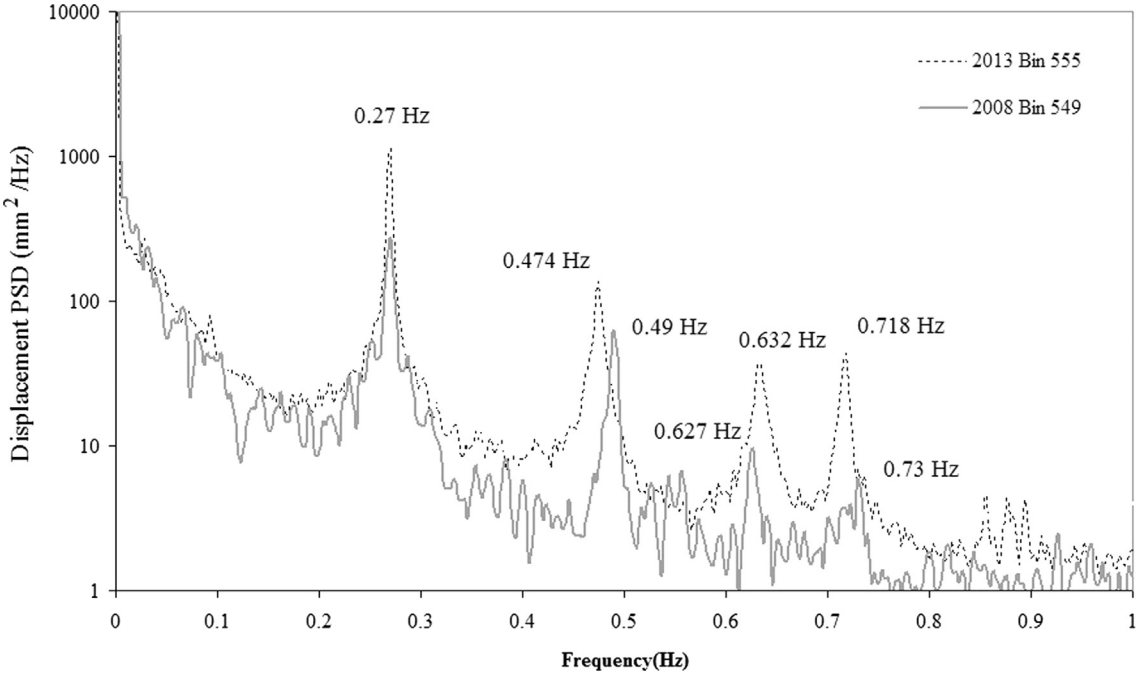

Fig. 7. Example of a power spectral density (PSD) calculated from data collected at different dates for two almost coincident bins. The solid line refers to the measurement configuration A1–08, bin 549, while the dashed line corresponds to C1–13, bin 555.

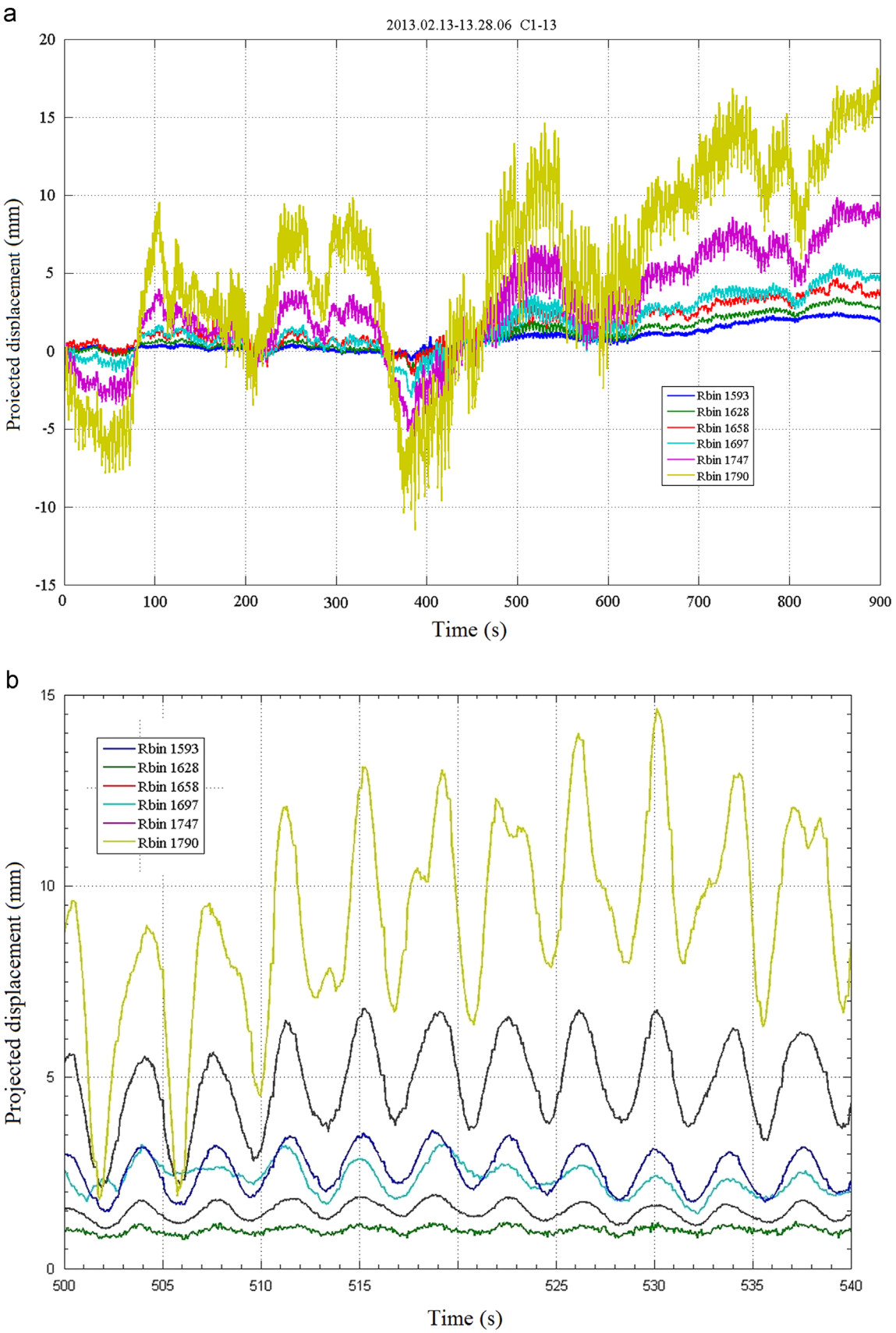

Fig. 8. Displacement time series retrieved from the measuring configuration C3–13 (top). Zoom of the interval 500–540 s of the same profile (bottom).

Table 3
Modal frequencies of the tower detected in three different experimental campaigns from 2008 to 2103.

Tower main detected frequencies (Hz)	A1–08 (2008)	B1–12 (2012)	C1–13 (2013)
f_0	0.270	0.268	0.270
f_1	0.490	0.474	0.474
f_2	0.627	0.628	0.632
f_3	0.730	0.710	0.718

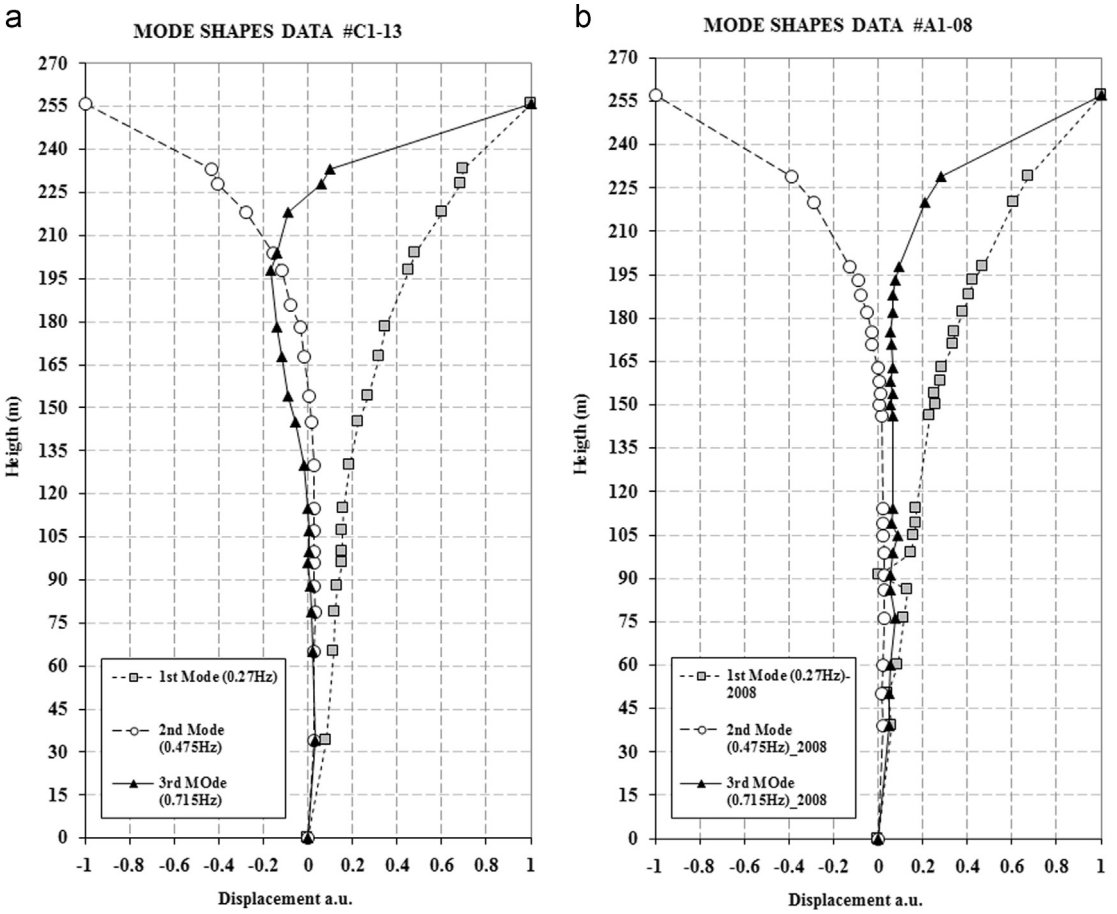

Fig. 9. Vibration modes identified through FDD technique [18] from the deflections measured during the A1–08(left) and C1–13 (right) data collection (see Table 1).

0.715 Hz, clearly shown in Fig. 9a and b respectively. Comparing the two plots, we observe that the modal shapes corresponding to the first two modes are very similar, while those one obtained for the third frequency does not reproduce exactly the same shape. This result can be related to the differences present in the spectra behaviour of the two acquisitions, shown as Fig. 7. Observing the two spectra, it can be noted that for the two lower frequencies, 0.27 Hz and 0.474/0.479 Hz, their amplitude during the two acquisitions was very similar; on the contrary, at 0.718/0.730 Hz the two peaks show a significant difference. The data, which show a more detailed modal shape, are those corresponding to the 2013 acquisition, when it was observed a higher intensity at the corresponding modal frequency.

4.4. Monitoring of the guys

A procedure to retrieve the tension forces of the cables was investigated taking advantage of the capability of radar to provide remote observations. The physical principle consists in measuring cable resonant frequencies and considering the cable as a taut string, obtaining the tension force from the detected natural frequencies. The dynamic behaviour of the stay cables of a large cable-stayed bridge, and a guyed mast, has been investigated using different approaches [19–22] in particular the use of radar apparatus has been proposed by Gentile et al. [23] and, Gentile and Ubertini [9] in 2010 and 2012, respectively. Bennet [24] applied the same technique to the monitoring of a pedestrian bridge.

According to this approximation the tension force T in the cable and the natural frequency, f_n, of the stay cables are related by the following formula:

$$T = 4L^2\rho\left(\frac{f_n}{n}\right)^2 \tag{2}$$

where L is the effective length of the cable (metres), ρ the mass per unit length (kg/metre), and n the integer index of the natural frequency, f_n (Hz). According to this approximation the structural parameters of the cable can be joined to a single factor K, rewriting Eq. (2) as follows:

$$T = K \cdot \left(\frac{f_n}{n}\right)^2 \tag{3}$$

where K is

$$K = 4L^2\rho \tag{4}$$

In the case at hand the procedure to estimate the tension force of the tower stays was carried out by means of the following steps: (1) acquisition of preliminary radar data to find the tower vibrating frequencies; (2) selection of the optimum radar position to obtain a strong signal from a cable, and where the actual vibration of the cable is along the LOS; (3) processing the displacement time series of the cable vibration to calculate the PSD of the bin corresponding to the stay-cable, to identify its main vibrating frequencies; (4) analysis of the spectra obtained through different observation geometries, to separate the contributions coming from the cables from those caused by the tower; and (5) calculation of the tension force T of the cable from its natural frequencies using Eq. (3). The geometry of the cable monitoring has been already introduced in Fig. 3, where a typical SNR radar range profile is also depicted.

An example of displacement time series is shown in Fig. 10 (configuration measurement B1–12, Table 2). The signal shows a clear periodicity, with a peak to peak amplitude that ranges from 80 to 140 mm. Fig. 11 shows the corresponding PSD (sub-sample=500 s, overlapping=66% and δF=0.002 Hz). Several main frequency peaks can be extracted: 0.268 Hz, 1.064 Hz, 2.132 Hz, 3.192 Hz, 4.264 Hz, 5.316 Hz, 6.354 Hz, and 7.452 Hz. Considering the outcomes from the tower vibration study, we were able to clearly distinguish, in the above series, the peak associated with the tower oscillation (0.268 Hz, 0.474 Hz) from the remainder ones that characterize the cable. This is essential to properly analyse the cable, thus deriving the tensions from frequencies.

We collected data on the same cable (G1–B2) using the different geometries depicted in Fig. 12. Table 4 resumes the first natural frequencies obtained and the PSD calculated from the different geometries are jointly plotted in Fig. 13. G1–B2 guy is composed of 158 strands. In Fig. 13 the frequencies associated to the tower are differently marked with respect to those from the cable. Focusing on the cable frequencies, it is worth noting that measured and expected values, see Table 4, are almost coincident for the first natural frequency f_0, confirming a good agreement with taut string approximation. Observing the frequencies detected for each measurement, there is a slow frequency drift with time, which will be discussed in the next paragraph.

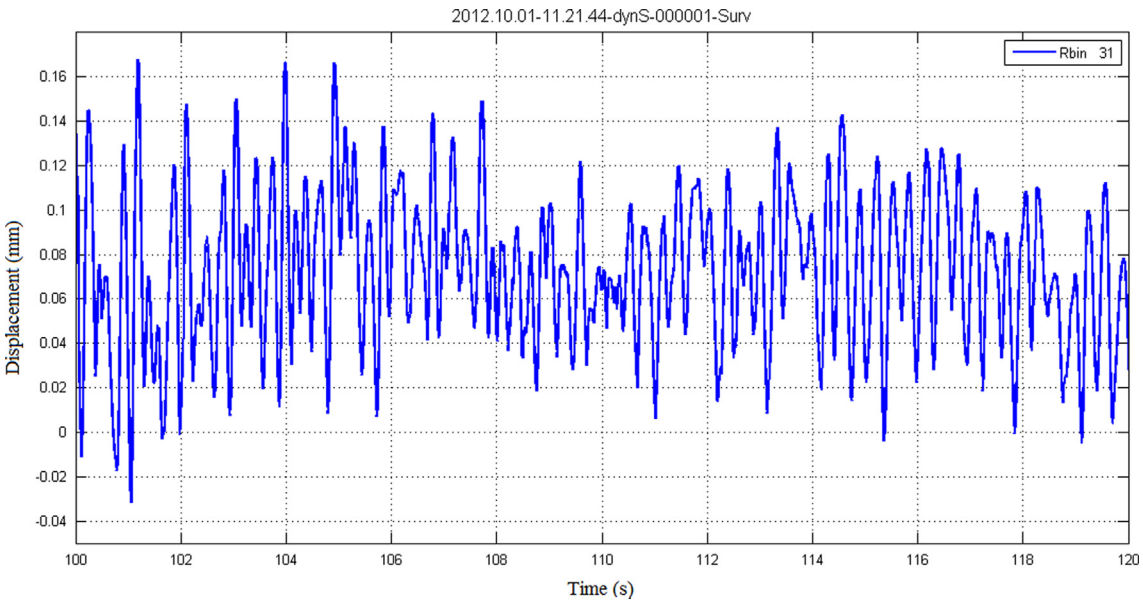

Fig. 10. Sample of 20 s extracted from the displacement time series measured through the radar observing cable G1 B1, corresponding to configuration B1–12.

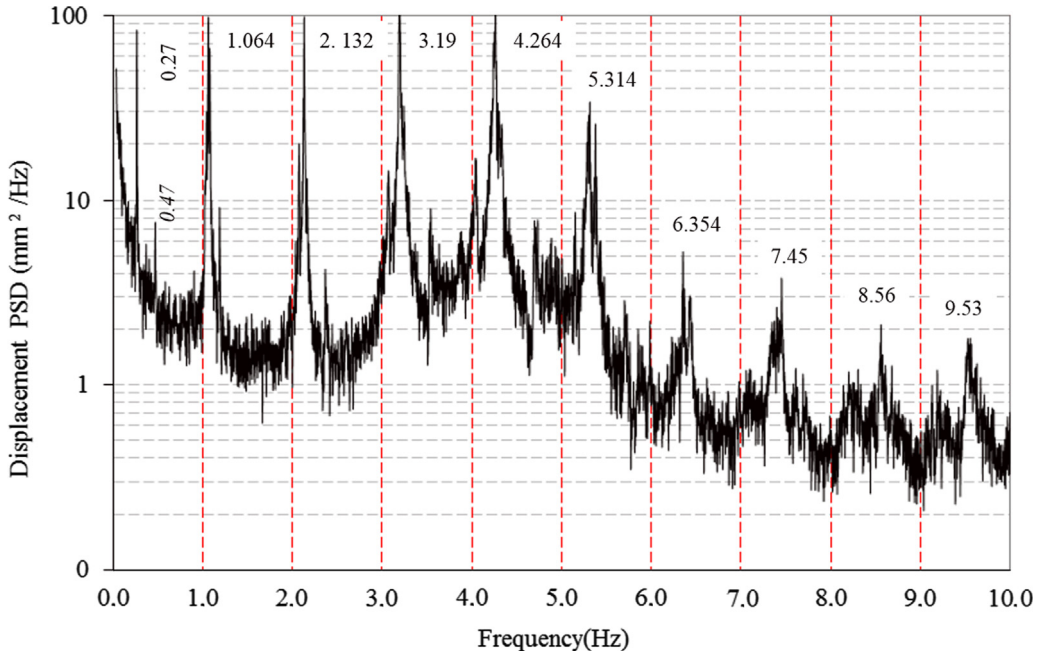

Fig. 11. Power spectral density (PSD) of the cable G1–B2, bin 31; duration=30 min; window=500 s; δF=0.002 Hz. The main detected peak values are at 0.27 Hz, 0.47 Hz (tower) and 1.066 Hz, 2.132 Hz, 3.190 Hz, 4.264 Hz, 5.316 Hz (cable).

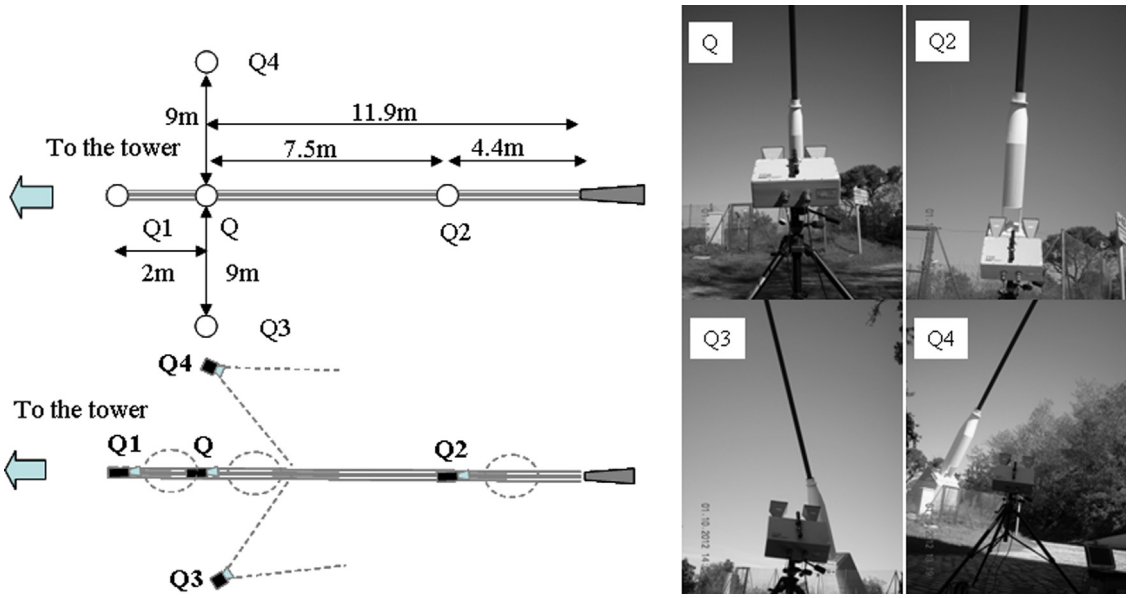

Fig. 12. Acquisition geometries during cable monitoring: to the left plane view of the radar location with respect to the cable (left). Photos of the corresponding data acquisition (right).

Table 4
Frequencies retrieved from radar measurements (grey columns) and expected values from tau string approximation formula.

Time GMT+2	Name	f_1	$f_1 \times 2$	f_2	$f_1 \times 3$	f_3	$f_1 \times 4$	f_4	$f_1 \times 5$	f_5	$f_1 \times 6$	f_6
11h21m	Q	1.066	2.132	2.132	3.198	3.190	4.264	4.264	5.330	5.316	6.396	6.354
11h57m	Q1	1.060	2.120	2.124	3.180	3.188	4.240	4.244	5.300	5.282	6.360	6.336
12h35m	Q2	1.056	2.112	2.112	3.168	3.166	4.224	4.218	5.280	5.256	6.336	6.312
13h18m	Q4	1.054	2.108	2.106	3.162	3.160	4.216	4.208	5.270	5.240	6.324	6.386
14h02m	Q3	1.050	2.100	2.100	3.150	3.150	4.200	4.194	5.250	5.226	6.300	6.270

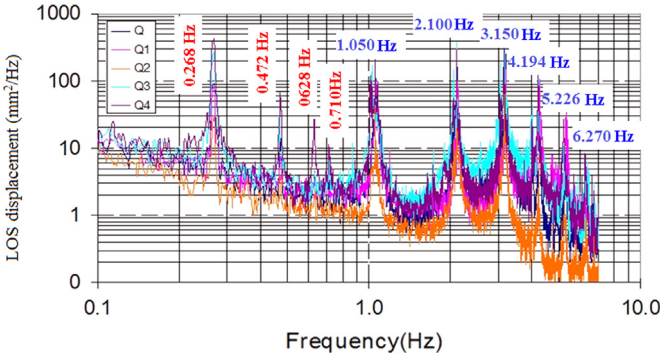

Fig. 13. Power spectral density calculated from radar data acquired monitoring the same cable from different geometries. Numbers vertically oriented indicate the frequencies related to the tower, horizontally oriented numbers refer to those from the cable (Q3).

Table 5
Frequencies retrieved from radar measurements, and expected values from tau string approximation formula. Acquisition date: 01.10.12.

Time GMT+2	Name	Measured f_1 (Hz)	Measured f_2 (Hz)	Measured f_3 (Hz)	Measured f_4 (Hz)
11h21m	Q	1.066	2.132	3.194	4.264
11h57m	Q1	1.060	2.124	3.188	4.244
12h35m	Q2	1.056	2.112	3.166	4.218
13h18m	Q4	1.054	2.106	3.160	4.208
14h02m	Q3	1.050	2.100	3.150	4.194

An in-depth analysis of Table 4 shows that the highest frequencies deviate a little (deviation $<1\%$) from the values expected from the taut string model approximation. Two types of phenomena are not considered in the taut string model: the sag extensibility of the cable and its bending stiffness [25]. The first effect introduces a negligible error for the higher modes, while the last can affect the higher frequency [24]. As far as these aspects are concerned, no specific increasing or decreasing trend is evidenced by these data, as expected because the calculated "Irving factor" λ^2 is $<<1$, largely within the value accepted for applying the tau string approximation [25].

The limited set of data does not allow a deeper analysis, so we estimate the tension force only using the first harmonics ($n=1$–4). To estimate the tension force, K (Eq. (4)) is calculated by means of ρ and L values provided by the Torre de Collserola SA: $\rho=206.3$ kg/m and $L=90.2$ m respectively and considering that the cable G1–B2 is composed of a 158 strands; the value for G1–B2 guy is $K=6718.0$ kN s^2. It is worth noting that we also approximate the effective length with the available real length. The results corresponding to the frequencies taken from Table 5 are reported in Table 6.

To better understand the occurrence of a noticeable shift of all the frequencies with time, the possible causes were investigated. We discard any instrumental effect because the stability of the radar was assessed with a huge amount of data collected in more than 5 years of experimental activities, and as confirmed by the high stability of the frequency detected for the tower in the campaigns here mentioned. Due to the potential sensitivity of cable tension with temperature we investigated the relationship between the measured frequency and the cable temperature, estimated through the air temperature. Each frequency, f_1–f_4, showed a high linear correlation with air temperature, with slope values very close.

Meteorological data have been obtained from the Fabra observatory (www.meteo.cat; Lat. 41.4183°N, Long. 2.1242°E, altitude 410 m). The station is located at a distance of 800 m from the tower and at the same altitude of the tower base. The data of Table 4 is plotted in Fig. 14, calculating for each natural frequency a regression line. A high correlation between the measured frequency and air temperature, for each order of frequency, $n=1$ to 4, is found; the obtained tension force/temperature coefficients are approximately 40 kN/ºC. For the sake of completeness, two aspects need to be mentioned. Although the actual temperature of the cable can be influenced by the different aspect direction with respect to the sun illumination, differing from that of the air, this relation seems indeed to confirm a high correlation. Secondly, a tension variation could also occur due to the mutated wind conditions. Wind velocity and direction were changing during data acquisition: the first oscillating within $\pm$ 2 m/s, while the second varied of about 50°, monotonically.

Due to the small temperature range available in the study at hand, this relationship cannot be applied for correcting the temperature effect on tension force estimates in general cases; a wider dataset is needed to confirm the value of this thermal coefficient. It is worth noting that a straightforward understanding of the cable behaviour also demands a deep analysis of the two phenomena cited previously, the sag extensibility of the cable, which can be directly influenced by the cable temperature [26], and the bending stiffness, which can reduce the application of the taut string model.

Table 6
Tension force calculated through the frequencies of Table 5.

Time GMT+2	Name	Calculated from *f*1 *T* (kN)	Calculated from *f*2 *T* (kN)	Calculated from *f*3 *T* (kN)	Calculated from *f*4 *T* (kN)	Average *T* (kN)	Standard deviation (%)
11h21m	Q	7634.03	7634.03	7614.95	7634.03	**7629.26**	0.1
11h57m	Q1	7548.34	7576.85	7586.36	7562.59	**7568.54**	0.1
12h35m	Q2	7491.48	7491.48	7482.02	7470.21	**7483.80**	0.1
13h18m	Q4	7463.13	7448.97	7453.69	7434.83	**7450.16**	0.1
14h02m	Q3	7406.59	7406.59	7406.59	7385.44	**7401.30**	0.1

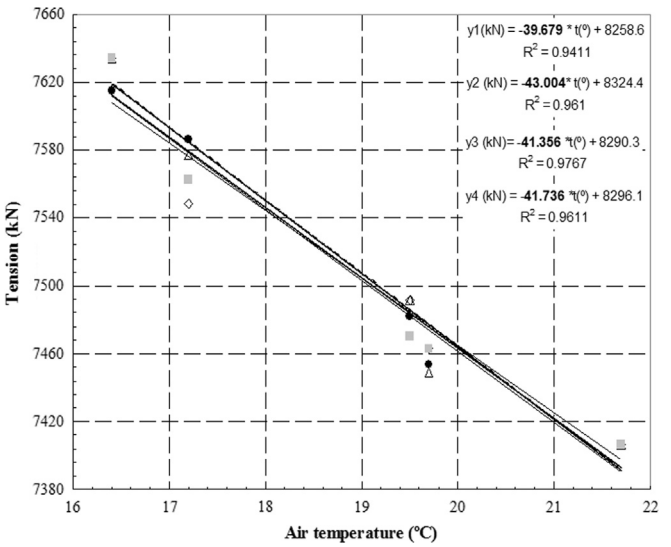

Fig. 14. Tension forces (kN) vs air temperature (°C). Regression lines are traced using data corresponding to the same order of natural frequencies, i.e. $n=1$, 2, 3, 4, but at different air temperatures.

5. Conclusion

The suitability of an interferometric radar to measure the dynamic response of a tall tower and of its stay cables, with high level of accuracy in terms of identification of natural frequencies, has been investigated on the bases of a wide set of experimental data. Four main vibration frequencies of the structure have been detected and three modal shapes have been identified. The robustness of the applied technique has been assessed using different geometrical configuration and data acquisition carried out at different dates along 5 years. The simultaneous acquisition of data from the tower and the cables allowed separating their different contributions. As far as the cables are concerned, the validity of the taut string approximation, restricting to their first natural frequencies, has been confirmed. The tension force of one of the cables has been estimated through a wide set of data. Based on an experimental analysis, a shift of the tension force of the cable has been identified and hence associated to variation of cable temperature. A tentative order of magnitude of this thermal effect has been estimated in approximately 40 kN per Celsius degree, although an ultimate assessment of this parameter demands a wider set of data, spanning a large range of temperatures, and the accurate examination of the limits of the applied taut string approximation.

Acknowledgements

Special thanks are due to Jesus Arasa Cugat for his valuable support during the experimental data collection. Torre Collserola SA is kindly acknowledged for hosting the experimental campaigns and providing structural data of the tower and the cables.

References

[1] M. Pieraccini, M. Fratini, F. Parrini, C. Atzeni, Dynamic monitoring of bridges using a high-speed coherent radar, IEEE TGRS 40 (11) (2006) 3284–3288. (Nov).
[2] C. Gentile, G. Bernardini, An interferometric radar for non-contact measurement of deflections on civil engineering structures: laboratory and full-scale tests, Struct. Infrastruct. Eng. 6 (5) (2010) 521–534, http://dx.doi.org/10.1080/15732470903068557.

[3] T.A. Stabile, A. Perrone, M.R. Gallipoli, R. Ditommaso, F.C. Ponzo, Dynamic survey of the Musmeci bridge by joint application of ground-based microwave radar interferometry and ambient noise standard spectral ratio techniques, IEEE GRSL 10 (4) (2013) 870–874, http://dx.doi.org/10.1109/LGRS.2012.2226428. (July).
[4] G. Luzi, O. Monserrat, M. Crosetto, The potential of coherent radar to support the monitoring of the health state of buildings, Res. Non-destruct. Eval. 3 (Issue 23) (2012) 125–145.
[5] C. Negulescu, G. Luzi, M. Crosetto, D. Raucoules, A. Roullé, D. Monfort, L. Pujades, B. Colas, T. Dewez, Comparison of seismometer and radar measurements for the modal identification of civil engineering structures, Eng. Struct. V. 51 (2013) 10–22.
[6] M. Pieraccini, F. Parrini, M. Fratini, C. Atzeni, P. Spinelli, In-service testing of wind turbine towers using a microwave sensor, Renew. Energy0960-148133 (1) (2008) 13–21. (*URL*).
[7] S. Rodelsberg, L. Wendolyn, C. Gerstenecker, M. Becker, Monitoring of displacements with ground-based microwave interferometer; IBIS-S and IBIS-L, J. Appl. Geodesy 4 (2010) 41–54. (DOI 101515/JAG.2010.005).
[8] C. Atzeni, A. Bicci, D. Dei, M. Fratini, M. Pieraccini, Remote survey of the leaning tower of Pisa by interferometric sensing, IEEE GRSL 7 (1) (2010) 185–189. (Jan).
[9] Gentile C., Ubertini F., Radar-based dynamic Testing and System identification of a Guyed Mast, in: Tenth International Conference on Vibration Measurements by Laser and Noncontact Techniques — AIVELA2012 Ancona, Italy 27–29 June 2012, ISBN 978-0-7354-1059-6 ISSN 0094-243X pp 318-325.
[10] La Torre de Collserola, Editor: Cayfosa-Quebecor Barcelona 2002 ISBN 84-607-4996-7 (In Spanish with a technical summary in English).
[11] D. Tarchi, E. Ohlmer, A. Sieber, Monitoring of structural changes by radar interferometry, Res. Nondestruct. Eval. 9 (no. 4) (1997) 213–225.
[12] C. Farrar, T.W. Darling, A. Migliorini, W.E. Baker, Microwave interferometer for non-contact vibration measurements on large structures, Mech. Syst. Signal Process. 13 (2) (1999) 241–253.
[13] M. Pieraccini, G. Luzi, D. Mecatti, L. Noferini, C. Atzeni, A microwave radar technique for dynamic testing of large structure, IEEE Trans. Microw. Theory Tech. 51 (No. 5) (2003) 1603–1609. (May).
[14] Coppi F., Gentile C. and Ricci P. A software tool for processing the displacement time series extracted from raw radar data, in: Proceedings of the Ninth International Conference on Vibration Measuerements by Laser and Non-contact Techniques, Ancona, Italy; 22–25 June 2010. (AIP Conference Proceedings 1253, E.P. Tomasini (Ed.)).
[15] K. Itoh, Analysis of the phase unwrapping problem, Appl. Opt. 21 (14) (1982) 2470. (July 15).
[16] G. Luzi, O. Monserrat, M. Crosetto; Real Aperture Radar interferometry as a tool for buildings vibration monitoring: limits and potentials from an experimental study, in: Tenth International Conference on Vibration Measurements by Laser and Noncontact Techniques — AIVELA2012 Ancona, Italy 27–29 June 2012, ISBN 978-0-7354-1059-6 ISSN 0094-243X pp 309-317.
[17] P.D. Welch, The use of fast Fourier transform for the estimation of power spectra: a method based on time averaging over short, modified periodograms, IEEE Trans. Audio Electroacoust. AU-15 (2) (1967) 70–73. (Jun).
[18] R. Brincker, L. Zhang, P. Andersen, Smart Mater. Struct. 10 (2001) 441–445.
[19] A. Cunha, E Caetano, Dynamic measurements on stay cables of cable-stayed bridges using an interferometry laser system, Exp. Tech. Am. Soc. Exp. Mech. (SEM) 23 (3) (1999) 38–43.
[20] E. Caetano, S. Silva, J. Bateira, A vision system for vibration monitoring of civil engineering structures, Exp. Tech. SEM 35 (No. 4) (2011).
[21] E. Caetano, Cable vibrations in cable stayed bridges, SED 9 (2007). (IABSE).
[22] E. Caetano, Á. Cunha, On the observation and identification of cable-supported structures, in: Proceedings of the Eighth International Conference on Structural Dynamics EURODYN 2011 Leuven, Belgium, 4–6 July 2011 available in ⟨ftp://ftp.fe.up.pt/pub/Pessoal/Dec/ecaetano/Cnd/vento/2012_pub/ci14.pdf⟩.
[23] C. Gentile, Deflection measurement on vibrating stay cables by non-contact microwave interferometer, NDT&E Int. 43 (2010) 231–240.
[24] Bennett Paul James, Structural health monitoring of a cable stayed pedestrian bridge with interferometric radar (Thesis for the Master of Science degree). Published by University of Colorado Denver. Auraria Library, 2012 available in: ⟨http://hdl.handle.net/10981/697⟩.
[25] M. Irvine, Cable Structures, MIT Press, 1981.
[26] F. Treyssède, Free linear vibrations of cables under thermal stress, J. Sound Vib. 237 (1-2) (2009) 1–8. (doi: 101016/J.JSV.2009.07.00).